# An Analytical Solution for the Inverse Kinematics of a Redundant 7DoF Manipulator with Link Offsets

Giresh K. Singh and Jonathan Claassens

*Abstract*— This work addresses the inverse kinematics problem for the 7 Degrees of Freedom Barrett Whole Arm Manipulator with link offsets. The presence of link offsets gives rise to the possibility of the in-elbow & out-elbow poses for a given end-effector pose and is discussed in the paper. A parametric solution for all possible geometric poses is generated for a desired end-effector pose (position and orientation). The set of possible geometric poses are completely defined by three circles in the Cartesian space. A method of computing the joint-variables for any geometric pose is presented. An analytical method of identifying a set of feasible poses for some joint-angle constraints is also addressed.

## I. INTRODUCTION

Manipulator forward kinematics deals with determining the end-effector position and orientation given the individual joint angles. The robot parameters are normally expressed in the Denavit-Hartenberg (D-H) convention as described in Spong et.al. [2]. The inverse kinematic problem is to find out the required joint variables, to achieve a specified end-effector position and orientation.

Many robots with 6 or less degrees of freedom (DOFs) are configured so that solving the inverse kinematic problem is analytical and thus fast. An example is the PUMA 560. At least six degrees of freedom are required so that the end-effector position (3 DOF) and the orientation (another 3 DOF) can be arbitrarily assigned in some workspace. If, however, the robot has more than 6 DOF then it is termed redundant and there may be many inverse kinematic (IK) solutions for a given end-effector configuration. Often, 7-DoF redundant manipulators IK problems are solved iteratively with methods that rely on the inverse Jacobian, pseudo-inverse Jacobian or Jacobian transpose [3]. These approaches are generally slow and sometimes suffer from singularity issues.

Some authors have come to the conclusion that no analytical IK solution exists for a 7 DOF robot like the Barrett WAM (whole arm manipulator) [1]. Vande Weghe et al [4] state "In fact, for manipulators with more than six links there is no closed-form solution to this problem, and even for manipulators with six or fewer links there may be an infinite number of configuration space states that result in the same workspace stat". Berenson et al [5] noted "However, for redundant robots such as the 7DOF WAM arm, there are a potentially infinite number of IK solutions for a given

Jonathan Claassens is with the Mobile Intelligent Autonomous Systems, CSIR Pretoria, RSA jclaassens@csir.co.za

G. K. Singh is with Flight Mechanics & Control Division, National Aerospace Laboratories, CSIR Bangalore, India gksingh@nal.res.in

end-effector transformation and no analytical algorithm can be used." In their cases they employed a pseudo-analytical approach by sampling one of the robot DOFs and solving the remaining 6 DOFs analytically. This provides a sampled set of the manipulator null space given a required end-effector configuration. The aforementioned IK solvers thus provide sampled or point solutions to the problem. This paper will show that there is, in fact, an analytical solution for the Barrett WAM's IK problem.

Dahm and Joublin presented a closed form solution for the IK problem of a 7 dof robot arm in [6]. This was done by treating each successive roll and pitch joints together as a spherical joint. The redundancy manifold was identified as a circle in the Cartesian space. Moradi & Lee [7] extended this formulation and worked out the limits for the redundancy angle parameter for the shoulder joint limits. Shimizu et al [8] proposed an IK solution for the PA10-7C 7DoF manipulator with arm angle as the redundancy parameter. They provided a detailed analysis of the variation of the joint angles with the arm angle parameter. This was then utilized to address redundancy resolution. However, link offsets were not considered in their work. Tarokh and Kim [9] include the link offsets, but their IK solution is based on decomposition of the work-space into cells and uses approximation techniques to find off-grid solutions.

A complete analytical solution for the Barrett WAM is not available in the open literature. Further, link offsets have not been addressed in the analytical IK approaches cited above. The contribution of this paper is an analytical solution to the IK problem for the 7 DOF Barrett WAM with link offsets explicitly considered. The presence of link offsets gives rise to the possibility of two poses (called as the in-elbow and the out-elbow poses) attaining the same workspace state, and is demonstrated in this paper. It is shown that all possible geometric poses can be completely defined by three circles in the Cartesian space. This can be parameterised by a single angle parameter running over one of the circles. The usable limits on the redundancy circle have also been determined for some of the joint variables. In this approach a specific solution can be selected from the null space of solutions through specification of the elbow position.

## II. BARRETT WAM & THE INVERSE KINEMATICS PROBLEM

The Barrett WAM is a 7 DOF manipulator that has only revolute joints. A schematic with all the joint variables is shown in Figure 1. The first two variables specify the azimuth (J1) and the elevation (J2) of the lower arm from the base

TABLE I

| $k$ | $a_k$ (m) | $\alpha_k$ (rad) | $d_k$ (m) | $\theta_k$ | Lower Limit ($\theta_{kL}$ rad) | Upper Limit ($\theta_{kU}$ rad) |
|---|---|---|---|---|---|---|
| 1 | 0 | $-\pi/2$ | 0 | $\theta_1$ | -2.6 | 2.6 |
| 2 | 0 | $\pi/2$ | 0 | $\theta_2$ | -2.0 | 2.0 |
| 3 | 0.045 | $-\pi/2$ | 0.55 | $\theta_3$ | -2.8 | 2.8 |
| 4 | -0.045 | $\pi/2$ | 0 | $\theta_4$ | -0.9 | 3.1 |
| 5 | 0 | $-\pi/2$ | 0.3 | $\theta_5$ | -4.76 | 1.24 |
| 6 | 0 | $\pi/2$ | 0 | $\theta_6$ | -1.6 | 1.6 |
| 7 | 0 | 0 | 0.06 | $\theta_7$ | -3.0 | 3.0 |

position. The third variable is a twist DOF of the lower arm (J3). The fourth variable corresponds to the forearm (upper arm) elevation (J4) from the joint, or elbow angle. The fifth and the sixth variables set wrist azimuth (J5) and elevation (J6) from the forearm. The seventh variable sets the hand rotation (J7).
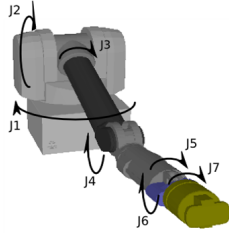


Fig. 1. Joints of the Barrett WAM

The forward kinematics for a manipulator is easily expressed in the D-H convention, which offers a simple way to find out the end-tool position and orientation, given the seven joint variables $[\theta_1, \theta_2, \theta_3, \theta_4, \theta_5, \theta_6, \theta_7]$. The DH parameters for the Barrett WAM are given in Table I. The homogeneous transformation matrix for a joint '$k$' is typically represented as $^{(k-1)}T_k$, and depends only on the $k^{th}$ joint variable. It is a $4 \times 4$ matrix, with the first $3 \times 3$ rotation sub matrix giving the orientation of the frame attached to that link, with respect to the $(k-1)^{th}$ frame and the three entries in the fourth column giving the position.

$$^{(k-1)}T_k = \begin{bmatrix} C\theta_k & -S\theta_k C\alpha_k & S\theta_k S\alpha_k & a_k C\theta_k \\ S\theta_k & C\theta_k C\alpha_k & -C\theta_k S\alpha_k & a_k S\theta_k \\ 0 & S\alpha_k & C\alpha_k & d_k \\ 0 & 0 & 0 & 1 \end{bmatrix}$$

(1)

where $C\theta_k$ and $S\theta_k$ represent $cos(\theta_k)$ and $sin(\theta_k)$ for the angle $\theta_k$ respectively.

The complete transformation matrix from the base to the end-tool is computed as

$$^0H_n = {}^0T_1^1T_2 \ldots {}^{(n-1)}T_n = \begin{bmatrix} R_n^0 & T_n^0 \\ 0 \ldots 0 & 1 \end{bmatrix}$$

(2)

Here, $R_n^0$ and $T_n^0$ give the rotated tool axes and the position in the base frame.

## A. The IK Problem

The inverse kinematics problem for a manipulator is defined as follows: Given a desired end-tool position vector $DT_{pos} = [T_x, T_y, T_z]$ in the inertial frame and a desired tool orientation described by the rotation matrix $DT_{orient} = [TR_x, TR_y, TR_z]$; find the joint variables $[\theta_1, \theta_2, \theta_3, \theta_4, \theta_5, \theta_6, \theta_7]$.

It should be further noted that the first four variables i.e. $[\theta_1, \theta_2, \theta_3, \theta_4]$ are involved in positioning the wrist, while the last three $[\theta_5, \theta_6, \theta_7]$ are used to get the desired tool-axis. The desired wrist position (DWpos) for this can be obtained as $DW_{pos} = DT_{pos} - TR_z * Tool\_Length$.

The joint angles can be computed if a complete geometric solution of the manipulator pose is known. The next section presents a method to obtain a parametric geometric solution to the wrist-positioning problem. The computation of the joint-angles for any pose is discussed in the following section. The last section addresses the issue of joint-angle constraints. A method of identifying a set of feasible poses considering constraints on some of the joint variables is discussed.

## III. ALL POSSIBLE POSES: A GEOMETRIC SOLUTION

The desired position of the wrist joint can be computed as discussed above. The lower arm and the upper arm links with their offsets are rigid bodies; with the elbow-joint between the two. If they were individually free to rotate i.e. the lower (upper) arm with the base (wrist-position) as centre, they could form two independent spheres. The set of possible poses would then be given by the intersection of these two spheres. It is obvious that the intersection set of the two spheres can be a circle, a point, or a null set. This is called as the "generating circle" (or a redundancy circle as in [6]). If the intersection is the null set; it implies that the specified wrist-position is not reachable.
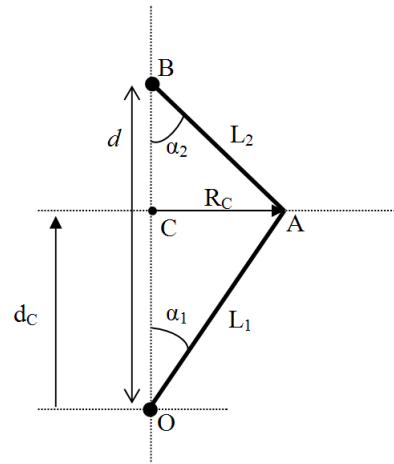


Fig. 2. The geometry for the intersection set

**Fact 1:** The upper & lower links are constrained to lie in the plane, which includes the base, the elbow, and the wrist joints, by construction.

It thus follows that the geometry of the intersection problem is invariant with respect to the orientation of the line joining the centres of the two spheres. The geometric solution for the possible poses is thus calculated with the normalized wrist position placed vertically above the base joint. Solutions for other orientations can be easily obtained by applying an appropriate normalizing rotation matrix.

The geometry of the "generating circle" can be easily computed. Given two links of length $L1$ (line OA) and $L2$ (line BA), separated by a distance '$d$' between them as shown in Figure 2. Then, the intersection set (denoted in the plane by the point $A$, or the elbow-joint) is described by the centre lying at point $C$, at a distance $d_C$ from point $O$ and the radius $R_C$ (line CA). The angles $\angle COA$ & $\angle CBA$ subtended by the intersection point A at the wrist position and the base from the vertical axis are represented by $\alpha_1$ and $\alpha_2$ respectively. From the geometry of the problem, these angles can be easily obtained as

$$\alpha_2 = cos^{-1}\left[(d^2 + L_2^2 - L_1^2)/(2dL_2)\right], \text{ and}$$
$$\alpha_1 = sin^{-1}\left[L_2 sin(\alpha_2)/(L_1)\right] \tag{3}$$

Further, the $d_C$ and $R_C$ follow as

$$d_C = L_1 cos(\alpha_1) = d - L_2 cos(\alpha_2) \text{ and}$$
$$R_C = L_1 sin(\alpha_1) = L_2 sin(\alpha_2) \tag{4}$$

It is obvious that if $\left[(d^2 + L_2^2 - L_1^2)/(2dL_2)\right] > 1$, no solutions are possible for $\alpha_2$, implying a null set condition. If a solution exists, then all possible poses for the manipulator arm are given by the circle of radius ($R_C$) centred at the point $C$, at a distance $d_C$ from the base.

The manipulator arm is not a straight link as assumed in the earlier computation or as in [8], but has link offsets. There are two possible solutions for each point on the circle, which is labelled as the out-elbow pose (see Figure 3) and the in-elbow pose (see Figure 4). These are called thus, because in the first case the upper & lower joints lie outside the generating circle. The position of the joints in the upper & lower arm (represented as points $U_J$ and $L_J$ in the figure) is required for a complete geometric pose. This is discussed in the following sub-sections. It should be noted that, the two links are constrained to lie in the same plane by construction. Hence the effect of these offset links can be easily incorporated in the in-plane analysis.

### A. Out-Elbow Pose

The out-elbow pose is shown in Figure 3. A radial outward vector ($O_{RAD}$) for the "generating circle" from the point $C$ is shown. The joint-location points $U_J$ ($L_J$) in the figure can be easily obtained by moving the offset-link distance along a up (down) rotated $O_{RAD}$. The magnitude of rotation can be easily seen from the figure as

$$\theta_U = \pi - (\pi/2 - \alpha_2) - \angle BAU_J, \text{ and}$$
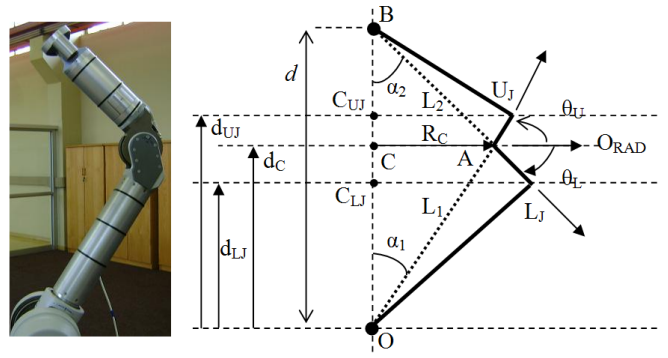$$\theta_L = \pi - (\pi/2 - \alpha_1) - \angle OAL_J \tag{5}$$



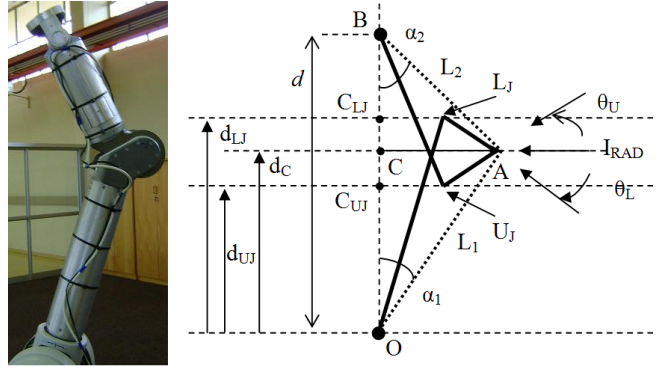Fig. 3.   The out-elbow pose geometry with the link offsets



Fig. 4.   The in-elbow pose geometry with the link offsets

The angles $\angle BAU_J$ and $\angle OAL_J$ are known from the given link and offset lengths as

$$\angle BAU_J = \pi/2 - tan^{-1}(a_3/d_3), \text{ and}$$
$$\angle OAL_J = \pi/2 - tan^{-1}(|a_4|/d_5) \tag{6}$$

### B. In-Elbow Pose

The in-elbow pose is shown in Figure 4. A radial inward vector ($I_{RAD}$) for the "generating circle" from the point $C$ is shown. The joint-location points $U_J$ ($L_J$) in the figure can be easily obtained by moving the offset-link distance along a down (up) rotated $I_{RAD}$. The magnitude of rotation can be easily seen from the figure as

$$\theta_U = \angle BAU_J - (\pi/2 - \alpha_2), \text{ and}$$
$$\theta_L = \angle OAL_J - (\pi/2 - \alpha_1) \tag{7}$$

### C. Summary

Since the upper & lower links are constrained to lie in the plane which includes the base, the elbow joint, and the selected wrist position, the upper & lower arm joint locations would also trace out a circle. These circles can be identified by the centres located at $C_{LJ}$ and $C_{UJ}$ located at distances $d_{LJ}$ and $d_{UJ}$ respectively from the base point $O$. The respective radii $R_{LJ}$ and $R_{UJ}$ are the distance of the line-segment $C_{LJ}L_J$ and $C_{UJ}U_J$ respectively. To summarize the earlier developments, for a given wrist-position, all possible poses are described by the following three circles, which can be readily obtained:

- The "generating circle" ($GC$) or the circle which describes the position of the elbow-joint: centred at point $C$ and radius $R_C$ at a distance $d_C$ from the base.
- The "upper-joint circle" ($UJC$): centred at point $C_{UJ}$ and radius $R_{UJ}$ at a distance $d_{UJ}$ from the base.
- The "lower-joint circle" ($LJC$): centred at point $C_{LJ}$ and radius $R_{LJ}$ at a distance $d_{LJ}$ from the base.

The geometric pose defined by the three circles can be easily parameterised using a single angle parameter on the $GC$. Let $C_{norm}(R, D, \phi)$ represent a normal circle of radius $R$ with its centre placed at a distance $D$ along the z-axis from the origin, with $\phi$ as a running parameter from $[-\pi, +\pi]$ as

$$
\begin{aligned}
C_{norm}(R, D, \phi) &= \begin{bmatrix} Rcos(\phi) & Rsin(\phi) & D \end{bmatrix} \\
&= \begin{bmatrix} RC\phi & RS\phi & D \end{bmatrix}
\end{aligned} \tag{8}
$$

Let the normalizing rotational matrix $R_{norm}$ (which places the desired wrist location to an equivalent normal position) be given as

$$
R_{norm} = \begin{bmatrix} r_{11} & r_{12} & r_{13} \\ r_{21} & r_{22} & r_{23} \\ r_{31} & r_{32} & r_{33} \end{bmatrix} \tag{9}
$$

Then the rotated circle is given as

$$
\begin{aligned}
C_{rot}(R, D, \phi) &= C_{norm}R_{norm} = \begin{pmatrix} C_{rot}(R, D, \phi)_x \\ C_{rot}(R, D, \phi)_y \\ C_{rot}(R, D, \phi)_z \end{pmatrix} \\
&= \begin{bmatrix} r_{11}RC\phi + r_{21}RS\phi + r_{31}D \\ r_{12}RC\phi + r_{22}RS\phi + r_{32}D \\ r_{13}RC\phi + r_{23}RS\phi + r_{33}D \end{bmatrix}
\end{aligned} \tag{10}
$$

This is illustrated by the following example.

**Example 1:** Let the desired end-tool position ($DT_{pos}$) be $[0.1, 0.1, 0.6]$ and the desired tool axis $TR_z$ be $[0.4959, 0.6393, -0.5877]$. The desired wrist position $DW_{pos} = DT_{pos} - 0.06TR_z = [0.0702, 0.0616, 0.6353]$. The computations are performed with $d = |DW_{pos}| = 0.6421$. The rotational matrix can be obtained as

$$
R_{norm} = \begin{bmatrix} 0.9940 & -0.0053 & 0.1094 \\ -0.0053 & 0.9954 & 0.0960 \\ 0.1094 & 0.0960 & 0.9894 \end{bmatrix} \tag{11}
$$

With the link-lengths as given in Table I, it is straight forward to get the three circles as $LJC \rightarrow [d_{LJ} = 0.4621; R_{LJ} = 0.2982]$, $GC \rightarrow [d_C = 0.4865; R_C = 0.2604]$, and $UJC \rightarrow [d_{UJ} = 0.5282; R_{UJ} = 0.2775]$. The computed poses and the three circles (rotated using $R_{norm}$) are shown in Figure 5. It is seen from the figure that the three circles describe all possible geometric poses for the problem.

## IV. ALL POSSIBLE SOLUTIONS: COMPUTATION OF THE JOINT ANGLES

It is seen from the previous section, that all possible poses for the IK Problem are described by the three circles, namely the $UJC$, the $GC$, the $LJC$, and the normalizing rotational matrix $R_{norm}$. However the desired solution for the IK problem is the set of joint variables: $[\theta_1, \theta_2, \theta_3, \theta_4, \theta_5, \theta_6, \theta_7]$. This section provides a method for finding these angles for
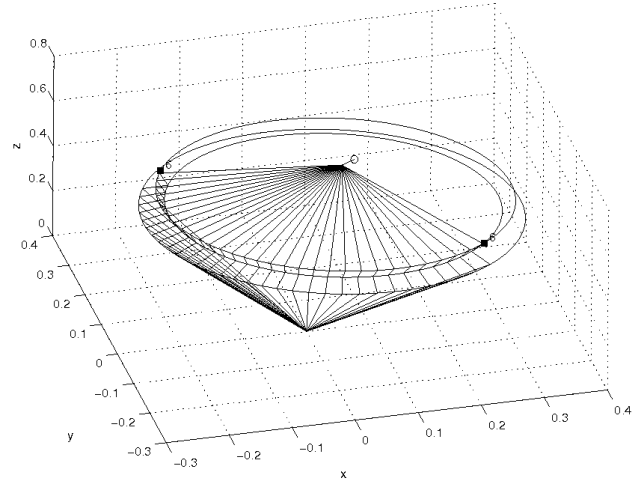


Fig. 5. The three Circles with the Computed Poses for Example 1

any given geometric pose. It should be restated that the three circles mentioned above are computed for the normalised wrist position. The actual pose corresponding to the actual wrist position has to be obtained by applying the rotation matrix $R_{norm}$ to any selected nominal pose.

Thus, it is assumed that the geometric pose is available in terms of the x-y-z coordinates of the following:

- Wrist position $DW_{pos} = [x_W, y_W, z_W]$,
- point $U_J = C_{rot}(R_{UJ}, D_{UJ}, \phi) = [x_{UJ}, y_{UJ}, z_{UJ}]$,
- point $A = C_{rot}(R_C, D_C, \phi) = [x_A, y_A, z_A]$, and
- point $L_J = C_{rot}(R_{LJ}, D_{LJ}, \phi) = [x_{LJ}, y_{LJ}, z_{LJ}]$.

The joint angles can be computed given the above geometric coordinates, as discussed here. The azimuth and the elevation of the lower arm from the base position can be computed as below

$$
\begin{aligned}
\theta_1 &= tan^{-1}(y_{LJ}, x_{LJ}), \text{ and} \\
\theta_2 &= cos^{-1}(z_{LJ}/d_3)
\end{aligned} \tag{12}
$$

It should be noted that the $tan^{-1}(.,.)$ is computed as the four-quadrant inverse tangent (as implemented in *Matlab* function $atan2(.,.)$).

The lower arm twist angle ($\theta_3$) can be computed from the normalised vector from the lower-arm joint to the elbow joint given by

$$
{}^{LJ}V_A = ([x_{LJ}, y_{LJ}, z_{LJ}] - [x_A, y_A, z_A]) / a_3 \tag{13}
$$

This corresponds to the x-axis of the homogeneous transformation ${}^0H_3 = {}^0T_1^1T_2^2T_3$. Equating the two gives:

$$
\begin{bmatrix} C\theta_1 C\theta_2 & -S\theta_1 \\ S\theta_1 C\theta_2 & C\theta_1 \\ -S\theta_2 & 0 \end{bmatrix} \begin{pmatrix} C\theta_3 \\ S\theta_3 \end{pmatrix} = {}^{LJ}V_A \tag{14}
$$

This makes a set of three equations in two unknowns. This can be solved for taking two equations at a time. Let the determinant for the first two equations be represented as

$D_{12}$, and so on. Then,

$$\begin{aligned} D_{12} &= C\theta_2, \\ D_{13} &= -S\theta_1 S\theta_2, \text{ and} \\ D_{23} &= C\theta_1 S\theta_2. \end{aligned} \quad (15)$$

It is easy to see that all three determinants cannot be simultaneously zero, hence one can always solve for the unknowns. The twist angle can then be computed as

$$\theta_3 = tan^{-1}(S\theta_3, C\theta_3) \quad (16)$$

The fourth variable corresponds to the forearm elevation from the joint, or also called as the elbow angle. This can be seen from Figure 3 and Figure 4 as

$$\begin{aligned} \theta_4 &= (\theta_U + \theta_L), \text{ for the out-elbow pose, and} \\ \theta_4 &= -(\theta_U + \theta_L), \text{ for the in-elbow pose.} \end{aligned} \quad (17)$$

It is seen that the $\theta_U$ and $\theta_L$ depend only on the normal distance $d$ between the base and the wrist-position, and the offset-link geometry. Thus the following fact follows.

**Fact 2:** The elbow angle is dependent only on the normal distance from the base to the wrist joint.

The fifth and the sixth variables provide for the wrist azimuth and the elevation. These angles can be computed as discussed below. Thus far the first four joint variables i.e. $[\theta_1, \theta_2, \theta_3, \theta_4]$ are known. These can be used to get the rotation matrix $R_4^0$ as below

$$^0H_4 = {}^0T_1^1T_2^2T_3^3T_4 = \begin{bmatrix} R_4^0 & T_4^0 \\ 0\ldots0 & 1 \end{bmatrix} \quad (18)$$

Given the wrist position ($DW_{pos}$) and the end-tool position ($DT_{pos}$), the coordinates of the end-tool in the local wrist-frame is obtained as:

$$\begin{pmatrix} x_{tool} \\ y_{tool} \\ z_{tool} \end{pmatrix} = \begin{bmatrix} R_4^0 \end{bmatrix}^T (DT_{pos} - DW_{pos}) \quad (19)$$

The azimuth angle ($\theta_5$) and the elevation angle ($\theta_6$) can then be obtained using the *Matlab* function $cart2sph$. Or equivalently,

$$\begin{aligned} \theta_5 &= tan^{-1}(y_{tool}, x_{tool}) + \pi, \\ \theta_6 &= tan^{-1}(z_{tool}, \sqrt{x_{tool}^2 + y_{tool}^2}) - \pi/2 \end{aligned} \quad (20)$$

for the out-elbow pose, and

$$\begin{aligned} \theta_5 &= tan^{-1}(y_{tool}, x_{tool}), \\ \theta_6 &= \pi/2 - tan^{-1}(z_{tool}, \sqrt{x_{tool}^2 + y_{tool}^2}) \end{aligned} \quad (21)$$

for the in-elbow pose.

The wrist elevation angle can equivalently be computed as the in-plane angle between the tool z-axis ($TR_z$) and the vector from the upper-joint to the wrist position.

The seventh variable provides for hand rotation. With the first six joint variables i.e. $[\theta_1, \theta_2, \theta_3, \theta_4, \theta_5, \theta_6]$ known, it is straightforward to get the rotation matrix $R_6^0$. The seventh joint angle can be easily obtained by the angle between this x

(y) axis and the desired tool orientation $TR_x$ ($TR_y$) respectively. The expressions for the joint angles obtained above are similar to the 'tangent' and 'cosine' type as reported in [8]. A detailed analysis of the joint-angle variation with respect to the redundancy parameter is presented in [8], and is hence omitted here. This section provides an analytical solution to the inverse kinematics problem for the 7-DoF Barrett WAM including the link offsets.

## V. FEASIBLE SOLUTIONS: JOINT ANGLE CONSTRAINTS

The previous section presented a method for finding the joint angles for any given geometric pose, for a desired end-tool position and orientation. However the joint angles are normally constrained to lie within specified lower and upper bounds. The upper and lower joint limits considered in [8] are quite restrictive as compared to those of the Barrett WAM (given in Table I). The following facts become important considering the large usable joint ranges in the WAM's case.

**Fact 3:** The homogeneous transformation matrix $^0H_7$ for joint variables $[\theta_1, \theta_2, \theta_3, \theta_4, \theta_5, \theta_6, \theta_7]$ is the same for the set $[\theta_1 \pm \pi, -\theta_2, \theta_3 \pm \pi, \theta_4, \theta_5, \theta_6, \theta_7]$.

**Fact 4:** The homogeneous transformation matrix $^0H_7$ for joint variables $[\theta_1, \theta_2, \theta_3, \theta_4, \theta_5, \theta_6, \theta_7]$ is the same for the set $[\theta_1, \theta_2, \theta_3, \theta_4, \theta_5 \pm \pi, -\theta_6, \theta_7 \pm \pi]$.

These can be easily established by comparing the $^0H_7$ for the sets of joint variables.

It can be seen from the Fact 3 and Fact 4 above, that for a given geometric pose, multiple solutions are possible for the joint variables. This section deals with the issue of finding the set of feasible poses in the parametric solution provided by the geometric solution. The joint-angle constraints can be computed as 'feasible' arcs on the three circles discussed previously. This would be very helpful in the manipulator path-planning problem.

The joint-angle computations outlined in the previous section can be used to establish the feasibility or otherwise of a possible pose. In the previous section, the coordinates of a possible pose were known and angles were being computed. Here the coordinates are represented parametrically in terms of the independent variable $\phi$, and solutions for the upper and lower constraints on the joint angles are sought for to obtain the 'feasible' arcs. The joint variables $[\theta_1, \theta_3, \theta_5, \theta_7]$ are seen to be of the 'tangent' type as in [8]. It can be easily seen that the full range of the tangent function is spanned by the ranges of these joint variables given in Table I. This is significantly different from the earlier work in [8], and hence the limits on the feasible arcs for these variables cannot be obtained. Getting feasible arcs for these variables is hence case-dependent, and has to be checked for separately. The 'feasible' arc computation for the remaining three variables $[\theta_2, \theta_4, \theta_6]$ is being presented in the following.

### A. Constraints on the Second Joint Variable ($\theta_2$)

The constraints on $\phi$ for the second variable can be determined from

$$(C_{rot}(R_{LJ}, D_{LJ}, \phi)/d_3) \geq cos(\theta_{2L}) = cos(\theta_{2U}) \quad (22)$$

## B. Constraints on the Fourth Joint Variable ($\theta_4$)

The fourth joint variable is the elbow angle and it depends only on the normal distance between the base joint and the wrist joint as discussed in Fact 2. From the earlier developments it is seen that the elbow angle for the out-elbow pose can be simplified to get

$$
\begin{aligned}
\theta_4 &= \theta_U + \theta_L, \\
&= (\alpha_1 + \alpha_2) + tan^{-1}(a_3/d_3) + tan^{-1}(|a_4|/d_5)
\end{aligned}
\tag{23}
$$

Then the possible minimum and maximum values for $(\alpha_1 + \alpha_2)$ can be obtained as

$$
\begin{aligned}
(\alpha_1 + \alpha_2)_{min} &= \theta_{4L} - \left[ tan^{-1}(a_3/d_3) + tan^{-1}(|a_4|/d_5) \right], \\
(\alpha_1 + \alpha_2)_{max} &= \theta_{4U} - \left[ tan^{-1}(a_3/d_3) + tan^{-1}(|a_4|/d_5) \right]
\end{aligned}
\tag{24}
$$

The normal distances for which these conditions would be met can be evaluated by applying the Lambert's cosine law for $\angle BAO$ in Figure 2.

$$
d = \sqrt{L_1^2 + L_2^2 - 2L_1 L_2 cos(\pi - (\alpha_1 + \alpha_2))}
\tag{25}
$$

The corresponding minimum and maximum values for the normal distance $d$ can be easily obtained as $0.2721m$ and $0.7343m$ respectively. It can be shown that the out-elbow poses are feasible only for $0.2721 \leq d \leq 0.8552$; and the in-elbow poses are possible only for $0.7343 \leq d \leq 0.8552$.

## C. Constraints on the Sixth Joint Variable ($\theta_6$)

As mentioned earlier, the wrist elevation angle can also be computed as the in-plane angle between the tool z-axis ($TR_z$) and the vector from the upper-joint to the wrist position. The normalized vector from upper-arm joint to the wrist position is given by

$$
{}^{UJ}V_{WP} = (C_{rot}(R_{UJ}, D_{UJ}, \phi) - DW_{pos})/d_5
\tag{26}
$$

The feasible range of $\phi$ can be computed from

$$
{}^{UJ}V_{WP} \odot TR_z \geq cos(\theta_{2L}) = cos(\theta_{2U})
\tag{27}
$$

where $\odot$ represents the dot-product.

The constraint equations for the second and the sixth joint variables can be simplified to get an equation of the form:

$$
asin(\phi) + bcos(\phi) = c
\tag{28}
$$

Where $a, b$, and $c$ can be easily derived. It should be noted that there will be either two solutions or no solution to this equation. There are no solutions if $|c/\sqrt{(a^2 + b^2)}| > 1$. In such cases the constraint will be either satisfied or not satisfied for the full range of $\phi$. This can be established by checking the constraint value for any one value of $\phi$.

The range of possible values of $\phi$ from the second and the sixth joint variables can thus be obtained using basic trigonometric operations. The feasible set for the arm pose will be given by the intersection of these two sets. It should be kept in mind that the constraints from the other variables
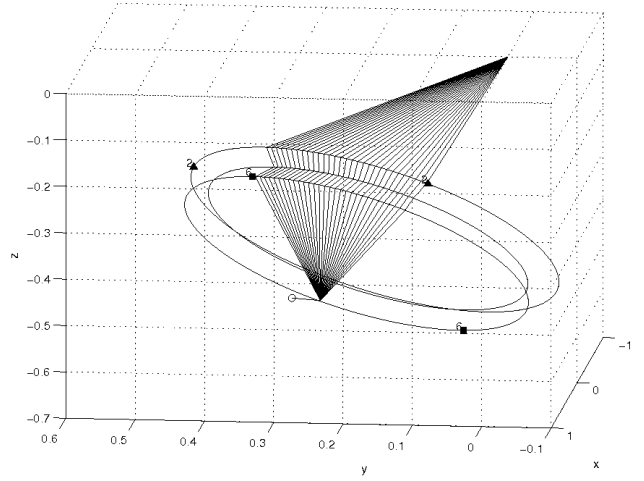


Fig. 6. Feasible Poses and possible $\phi$ ranges for Example 2

have not been considered; hence the actual set of feasible poses could be subset of this set. This is illustrated in the following examples.

## D. Examples

**Example 2:** Let the desired end-tool position ($DT_{pos}$) be $[0.3, 0.3, -0.5]$ and the desired tool axis $TR_z$ be $[-0.7071, 0.7071, 0]$. Then, $|DW_{pos}| = 0.6585$. The three generating circles, the set of feasible poses and the valid $\phi$ ranges are shown in Figure 6. The $\phi$ range obtained for the second joint variable is shown in 'filled triangles', while those for the sixth variable is shown in 'filled-squares'. The set of manipulator poses is generated using the joint-angle computation scheme presented earlier. It is seen that the set of feasible poses is the intersection set of the $\phi$ constraints from the second and sixth variables.

**Example 3:** Let the desired end-tool position $DT_{pos} = [0.3, 0.1, 0.3]$ and the desired tool axis $TR_z = [0, 0, 1]$. Then, $|DW_{pos}| = 0.3970$. The results are shown in Figure 7. There was no $\phi$ solution for the second joint variable and a point check showed that the constraint is always satisfied. The $\phi$ range for the sixth variable is shown in 'filled-squares'. The set of manipulator poses is generated as earlier. It is seen that the set of feasible poses is a subset of the $\phi$ constraints from the second and sixth variables. It is however observed that the set of feasible poses turns out to be a disjoint set. This is due to the fact that the first and third joint variables exceed their limits.

## VI. CONCLUSIONS AND FUTURE WORKS

### A. Conclusions

An analytical solution to the inverse kinematics problem for the 7 Degrees of Freedom Barret Whole Arm Manipulator with link offsets is presented. A method to obtain all possible geometric poses (both the in-elbow & out-elbow) for a desired end-effector position and orientation is provided. The set of geometric poses is completely determined by three circles in the Cartesian space. The joint-variables can
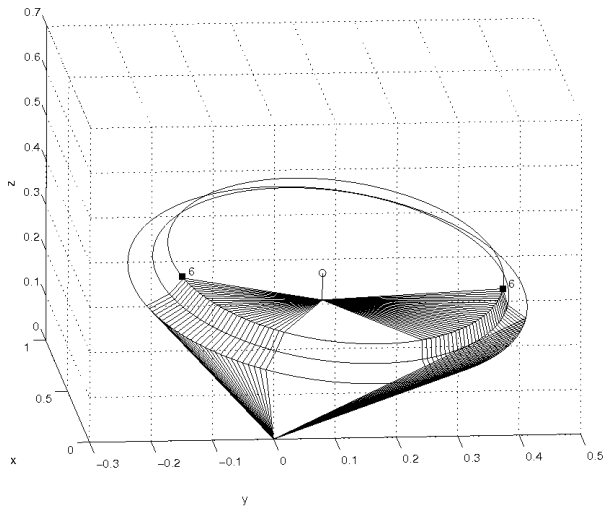
Fig. 7.   Feasible Poses and possible $\phi$ ranges for Example 3

be easily computed for any geometric pose. The physical constraints on the joint-angles restrict the set of feasible poses. The constraints on the set of feasible poses have been analytically worked out for the joint-variables of the 'cosine' type. It is also shown that the constraints for the remaining joint variables (which are of the 'tangent' type) cannot be generically computed for the 7 DOF Barrett manipulator. This would help in restricting the search domain for feasible poses during path planning.

*B. Future Work*

The presented inverse kinematics solution will be integrated into an RRT planner to optimize the planner's search through the configuration space.

## VII. ACKNOWLEDGMENTS

## REFERENCES

[1] www.barrett.com, Barrett Technology Inc., last accessed on the 7th of July 2010.
[2] M.W. Spong, S. Hutchinson, and M. Vidyasagar, *Robot Dynamics and Control*, John Wiley & sons Inc., 1989.
[3] L. Sciavicco and B. Siciliano, *Modelling and Control of Robot Manipulators* , Springer Second edition, 2000, Chapter 3, pp. 96.
[4] M. Vande Weghe, D. Ferguson, and S.S. Srinivasa, "Randomized Path Planning for Redundant Manipulators with Inverse Kinematics", *in IEEE-RAS International Conference on Humanoid Robots*, Nov. 2007.
[5] D. Berenson, S.S. Srinivasa, D. Ferguson, A. Collet, and J.J. Kuffner, "Randomized Path Planning for Redundant Manipulators with Inverse Kinematics", *in 2009 IEEE Conference on Robotics and Automation*, ICRA 2009.
[6] P. Dahm and F. Joublin, *Closed Form Solution for the Inverse Kinematics of a Redundant Robot Arm*, Institut for Neuroinformatik, Ruhr University, Bochum, Internal Report IRINI 97-08, 1997.
[7] H. Moradi and S. Lee, "Joint Limit Analysis and Elbow Movement Minimization for Redundant Manipulators using Closed Form Method", *in Advances in Intelligent Computing, Lecture Notes in Computer Science*, Vol. 3645 (2005), pp- 423-432.
[8] M. Shimizu, H. Kakuya, W. Yoon, K. Kitagaki, and K. Kosuge, "Analytical Inverse Kinematic Computation for 7-DOF Redundant Manipulators with Joint Limits and its application to Redundancy Resolution", *IEEE Trans. On Robotics*, vol. 24, No. 5, Oct. 2008.
[9] M. Tarokh and M. Kim, "Inverse Kinematics of 7-DOF Robots and Limbs by Decomposition and Approximation", *IEEE Trans. On Robotics*, vol. 23, No. 3, June 2007.